The Journal of Chemical Physics

Vibrationally inelastic scattering of HCl from Ag(111)

Cite as: J. Chem. Phys. **153**, 164703 (2020); https://doi.org/10.1063/5.0026228
Submitted: 22 August 2020 . Accepted: 30 September 2020 . Published Online: 22 October 2020

Jan Geweke, and Alec M. Wodtke

The Journal of Chemical Physics ARTICLE scitation.org/journal/jcp

Vibrationally inelastic scattering of HCl from Ag(111)

Cite as: J. Chem. Phys. 153, 164703 (2020); doi: 10.1063/5.0026228
Submitted: 22 August 2020 • Accepted: 30 September 2020 •
Published Online: 22 October 2020

Jan Geweke[1,2,3] and Alec M. Wodtke[1,2,3,4,a)]

AFFILIATIONS

[1] Department of Dynamics at Surfaces, Max Planck Institute for Biophysical Chemistry, 37077 Göttingen, Germany
[2] Max-Planck-EPFL Center for Molecular Nanoscience and Technology, Institute of Chemical Sciences and Engineering (ISIC), Station 6, École Polytechnique Fédérale de Lausanne, CH-1015 Lausanne, Switzerland
[3] Institute for Physical Chemistry, Georg-August University of Göttingen, 37077 Göttingen, Germany
[4] International Center for Advanced Studies of Energy Conversion, Georg-August University of Göttingen, 37077 Göttingen, Germany

[a)] **Author to whom correspondence should be addressed:** alec.wodtke@mpibpc.mpg.de

ABSTRACT

Using molecular beam cooled samples and quantum state-selective detection, we observe $v = 0 \rightarrow 1$ vibrational transitions when HCl ($v = 0$) collides with an Ag(111) surface and derive both the incidence energy and surface temperature dependence of the transition probability. Our observations reveal that both electronically adiabatic and non-adiabatic mechanisms are at play in this inelastic process. A comparison to other systems shows similarities and trends that are consistent with an electron transfer mechanism forming a transient HCl^{-}. For example, the electronically nonadiabatic coupling is stronger than for HCl scattering from Au, where the solid's work function is higher. HCl differs from other systems in that dissociation is possible over a low barrier. Vibrationally inelastic $v = 1 \rightarrow 2$ transitions could not be seen when HCl ($v = 1$) collides with an Ag(111) surface. We suggest that scattering events, where HCl ($v = 1$) is subject to dynamical influences that increase its vibrational energy, lead efficiently to dissociation before the HCl ($v = 2$) molecule can escape the surface. This system appears to be an excellent candidate to study electronically nonadiabatic effects in dissociative adsorption.

INTRODUCTION

The Born–Oppenheimer approximation (BOA), introduced almost a century ago,[1] still forms the basis of the majority of theoretical treatments of chemistry. However, over the past 3–4 decades, experimentalists have found copious evidence of the breakdown of the BOA in molecular interactions at metal surfaces. Vibrational promotion of electron emission[2] detects BOA failure directly as do chemicurrents.[3–6] Furthermore, BOA failure is responsible for H atom adsorption at metal surfaces.[7–10] Molecular dynamics simulation using electronic friction to characterize BOA failure successfully reproduced translational inelasticity of H and D collisions at metal surfaces as well as the magnitude of the isotope effect in chemicurrent experiments.[10]

There is strong evidence for BOA failure in vibrationally inelastic scattering of diatomic molecules colliding at noble metal surfaces—see work on NO/Ag(111),[11–14] NO/Cu(110),[15] NO/Au(111),[16,17] CO/Au(111),[18–21] N_2/Pt(111),[22] and CO/Ag(111).[23] The magnitude of the electronically nonadiabatic interaction is believed to be enhanced when a transient negative ion can be formed.[24] The key quantities that determine the energetics of transient anion formation are the solid's work function and the molecule's vertical electron binding energy, which is related to its electron affinity.[23] Another important question is how close the molecule can approach the surface, as image charge stabilization of the anion decreases with distance from the surface. Thus, incidence translational energy enhances electronically nonadiabatic vibrational excitation, even

though direct translational to vibrational energy transfer is unimportant.

Transient anion formation also appears to occur for vibrationally inelastic scattering of HCl from metals.[26,27] However, unlike for NO^- and CO^-, formation of HCl^- more easily leads to dissociation: $HCl + e^- \rightarrow H + Cl^-$ is only endoergic by 0.85 eV.[25] Furthermore, the van der Waals radius of Cl is ~0.2 Å larger than that of N or O.[26] Thus, the distance of closest approach may be substantially larger for this molecule limiting the image charge stabilization. Hence, it is not surprising that vibrationally inelastic scattering of HCl on Au(111) exhibits some differences to NO or CO scattering from noble metals.

For vibrationally inelastic scattering of HCl from Au(111), both electronically adiabatic as well as nonadiabatic interactions are evident,[26,27] whereas for NO and CO, only electronically nonadiabatic interactions are seen.[16–20] Furthermore, the probability for HCl ($v = 1 \rightarrow 2$) is ~20 times larger than that for HCl ($v = 0 \rightarrow 1$); by contrast, the probability for NO ($v = 2 \rightarrow 3$) is only 2× larger than NO ($v = 0 \rightarrow 1$).[27] The peculiarities seen for HCl inelastic scattering from Au(111) are likely due to the influence of electronically nonadiabatic interactions in the vicinity of a dissociative transition state.[27]

In this work, we extend our study to investigate the vibrational inelastic scattering of HCl from Ag(111), where the work function is 0.8 eV lower than that of Au.[28] We find evidence of strong adiabatic and nonadiabatic interactions. Furthermore, the $v = 0 \rightarrow 1$ vibrational excitation probabilities are similar in magnitude to those seen for HCl scattering from Au(111). The electronically nonadiabatic contribution to the vibrational inelasticity is 45% stronger for Ag(111) compared to Au(111), consistent with a mechanism involving transient negative ion formation that is sensitive to the solid's work function. Unlike for Au, we are unable to observe HCl ($v = 1 \rightarrow 2$) transition when scattering from Ag(111). This suggests that vibrational promotion of HCl dissociative adsorption is more important on Ag than on Au.

EXPERIMENTAL

The molecular beam surface-scattering apparatus has been previously described.[17,27,29] Briefly, it consists of four differentially pumped chambers. In the source chamber, a gas mixture of HCl seeded in H_2 was expanded either from a home-built, piezo- or solenoid-driven pulsed valve with either 2 or 8 bar stagnation pressure, respectively (298 K operating temperature). After passing through a 1.5 mm diameter skimmer and two differential pumping chambers with 3 mm and 2 mm diameter apertures, respectively, the molecular beam entered the ultra-high vacuum scattering chamber (base pressure ~2×10^{-10} Torr). The (111) surface (orientation accuracy better than 0.1°, purity 99.999%, MaTeck GmbH) of an Ag single crystal was positioned ~180 mm away from the nozzle and was mounted on a 4-axis (x, y, z, Θ) translation stage. The surface was prepared daily by sputtering with Ar ions (3 keV, 30 min), followed by annealing at 900 K for ~60 min. The cleanliness of the surface was checked using Auger electron spectroscopy. HCl pulses were analyzed prior to collision 15 mm in front of the Ag(111) surface—they were ~40 μs (FWHM) in duration. By changing the HCl/H_2 mixing ratio, the mean incidence energy of the HCl molecules was varied between 0.66 eV and 1.15 eV.

Populations of both vibrational states of HCl (v = 0,1) were measured after scattering from the Ag(111) surface by recording all observable ro-vibronic lines associated with the Q branch of the $E^1\Sigma^+ \leftarrow X^1\Sigma^+$ electronic band using a (2 + 1) Resonance Enhanced Multi-Photon Ionization (REMPI) scheme. Ion signals amplified by two Multi-Channel Plates (MCPs) in Chevron configuration were recorded for H^+, Cl^+, and HCl^+ and corrected for differences in MCP gain and variations in laser power.[17,27]

Information about incidence translational energy distributions was obtained using the state-to-state time-of-flight technique,[30] where incident HCl ($v = 0$, $J = 0$) molecules were excited to the $v = 1$, $J = 1$ state by laser generated IR light pulses. HCl in $v = 1$, $J = 1$ was subsequently ionized by REMPI—the pulsed REMPI laser beam ran parallel to the IR light beam but crossed the molecular beam ~30 mm further away. The REMPI signal was then recorded as a function of the delay between the two laser pulses.

We used an IR laser light source both for state-to-state time-of-flight and to investigate the vibrational excitation of HCl ($v = 1$). The IR laser system used a continuous wave (cw) Nd:YLF laser (Coherent Verdi V10) pumping a cw dye ring laser (Sirah Matisse DR, <20 MHz linewidth), whose output (~630 nm) was pulse-amplified in a five-stage Sirah pulsed amplifier. The pulsed visible light was combined with the fundamental output (1064 nm) of an injection seeded Nd:YAG laser (Spectra-Physics Quanta Ray Pro 230) for difference frequency mixing in a $LiNbO_3$ crystal. The mid-IR output was parametrically amplified with the Nd:YAG fundamental to give IR pulses at a wavelength of ~3.4 μm with energies of ~5 mJ to 7 mJ (see Ref. 31 for further information). In the absence of IR pre-excitation, only HCl ($v = 0$) could be detected in the incident molecular beam.

RESULTS

Figure 1 shows representative REMPI spectra of HCl molecules scattered into $v = 0$ [panels (a)–(c)] and $v = 1$ [panels (d)–(f)] by collisions at the Ag(111) surface held at three different temperatures. For the data in this figure, $\langle E_i \rangle$, the mean HCl translational energy of incidence, was 0.66 eV. Similar to the observations for HCl scattering from Au(111),[27] the intensity of the HCl ($v = 0$) REMPI signal decreases only slightly with an increase in surface temperature, while the REMPI signal from HCl ($v = 1$) is strongly enhanced.

We obtained and analyzed spectra like these at four values of $\langle E_i \rangle$ between 0.66 eV and 1.15 eV and T_s = 350 K–900 K. Integrating the REMPI spectra is the first step to finding the relative populations in both vibrational states represented by the spectra. We also applied corrections for differences in the experimental conditions such as detector gain, laser power, and angular and temporal distributions of the scattered flux and intrinsic properties like Franck–Condon factors, rotational line strengths, and ionization cross sections (cf. Refs. 17 and 27). Finally, the excitation probabilities, $P_{0,1}$, were calculated using Eq. (1) as the ratio of the number of $v = 0 \rightarrow 1$ transitions divided by all possible channels,

$$P_{0,1} = \frac{N_{0\rightarrow1}}{\sum_i N_{0\rightarrow i}} \approx \frac{N_{0\rightarrow1}}{N_{0\rightarrow0} + N_{0\rightarrow1}} \approx \frac{N_1}{N_0 + N_1}. \quad (1)$$

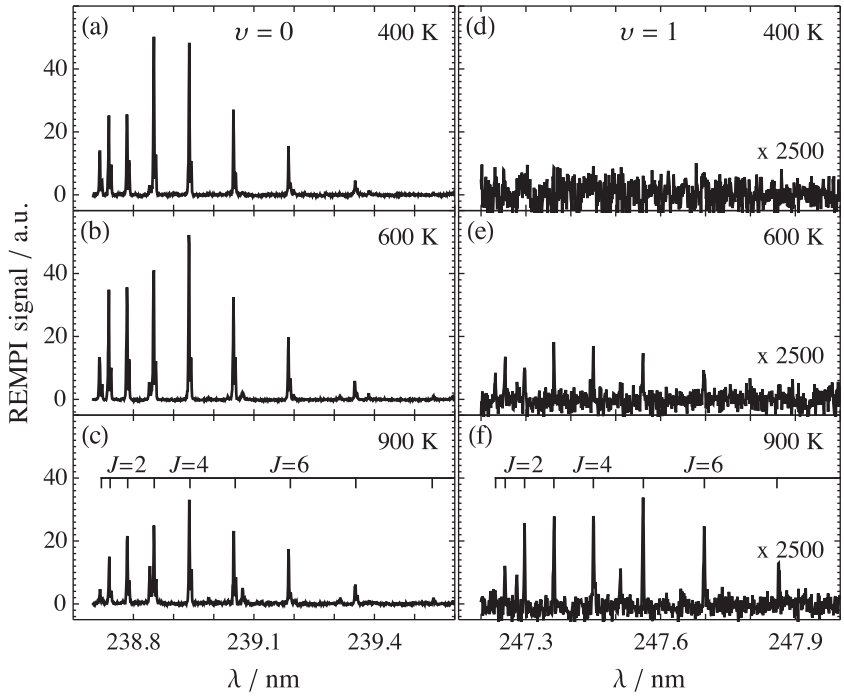

FIG. 1. Representative REMPI spectra of HCl molecules scattered from Ag(111) at three different surface temperatures. Shown are spectra probing HCl $\upsilon = 0$ [(a)–(c)] and $\upsilon = 1$ [(d)–(f)] recorded at $\langle E_i \rangle = 0.66$ eV that have already been corrected for differences in laser power. The relative scale is the same for all six panels. The spectra probing $\upsilon = 1$ are magnified by a factor of ~2500 relative to the spectra for $\upsilon = 0$. Additional lines not assigned to a certain J state belong to different transitions via the $V^1\Sigma^+$ state.

We assume that HCl dissociation is negligible[32] and that there is no excitation into higher vibrational states. Hence, $P_{0,1}$ is given by the ratio of the corrected population in $\upsilon = 1$, N_1, divided by the sum of populations in $\upsilon = 0$ and 1, N_0 and N_1.

Figure 2(a) shows the complete set of derived $P_{0,1}$ values. Both the surface temperature and incidence translational energy enhance the vibrational excitation, similar to the observations for HCl scattered from Au(111)[27,33] and other molecule/surface systems.[11,12,16,17,19,20,22,33]

The results of Fig. 2(a) can be fitted with Eq. (2),

$$P_{0,1}(E_i, T_s) = A_{0,1}^{ad.}(E_i) + A_{0,1}^{nonad.}(E_i)\exp\left(-\frac{E_{0,1}}{k_B T_S}\right), \quad (2)$$

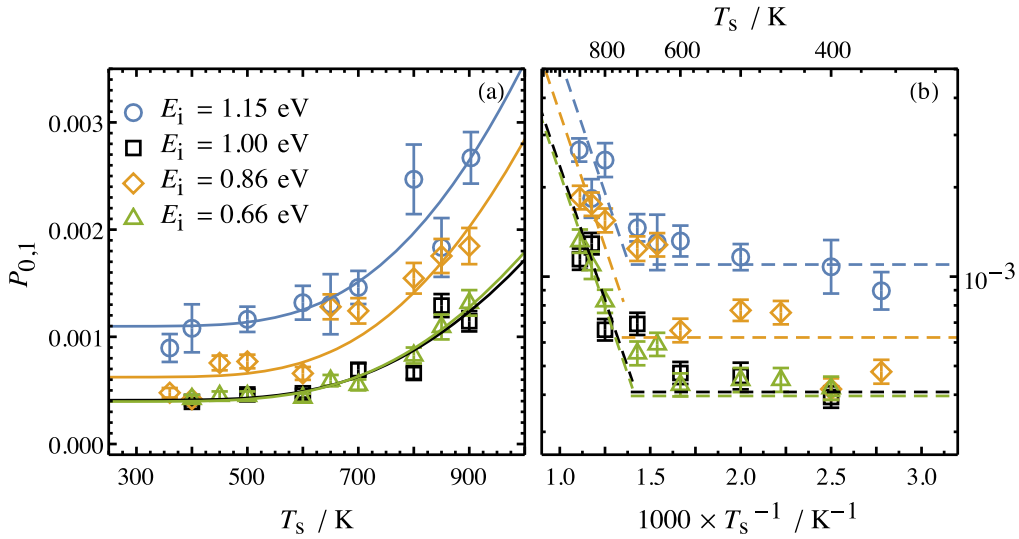

FIG. 2. Vibrational transition probabilities for $\upsilon = 0 \rightarrow 1$ when HCl molecules are scattered from Ag(111). Both increased surface temperature and incidence translational energy enhance the vibrational excitation probability. In panel (a), solid lines depict fits to the data according to Eq. (2). Panel (b) shows the exponential temperature dependence typical of electronically nonadiabatic coupling to excited electron–hole pairs and temperature independent behavior typical of electronically adiabatic T–V vibrational excitation.

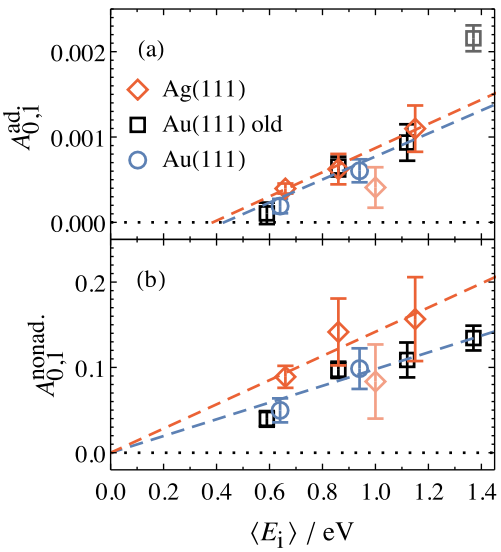

FIG. 3. Decomposition of the (a) adiabatic and (b) nonadiabatic interaction strength represented by $A_{0,1}^{ad.}$ and $A_{0,1}^{nonad.}$, respectively. Results are shown for $v = 0 \rightarrow 1$ excitation on Ag(111) and Au(111)[27,33] plotted against the incidence energy $\langle E_i \rangle$. The dashed lines are linear fits, whose slopes represent the interaction strengths. Note that the semitransparent data at $\langle E_i \rangle = 1.00$ eV were omitted for this fitting. In panel (a), thresholds for vibrational excitation can be derived from the simple linear fits—$0.39^{+0.05}_{-0.08}$ eV for HCl on Ag(111) and $0.43^{+0.11}_{-0.19}$ eV for HCl on Au(111). These values are both close to the $v = 0 \rightarrow 1$ energy spacing of 0.36 eV. See Ref. 27 for the explanation why we differentiate between old and new data on Au(111).

which reflects an electronically adiabatic influence that is independent of the surface temperature[34] and an electronically nonadiabatic influence with a characteristic Arrhenius-like surface temperature dependence.[12,15,17,20] The solid lines in Fig. 2(a) show the fit of Eq. (2), from which we derived $A_{0,1}^{ad.}(E_i)$ and $A_{0,1}^{nonad.}(E_i)$. Note that $E_{0,1}$ is not a fitting parameter; it is the vibrational excitation energy for HCl ($v = 1$).

The $\langle E_i \rangle$ dependence of $A_{0,1}^{ad.}(E_i)$ and $A_{0,1}^{nonad.}(E_i)$ is shown in Fig. 3, along with data obtained for the $v = 0 \rightarrow 1$ excitation of HCl on Au(111).[27,33] Both electronically adiabatic and nonadiabatic induced vibrational excitations of HCl are enhanced on silver compared to gold. We also note that, for both Ag and Au, the energy threshold of the adiabatic contribution, $\langle E_i \rangle = 0.39^{+0.05}_{-0.08}$ eV, is quite close to the vibrational spacing of the $v = 0 \rightarrow 1$ transition ($\Delta E_{v=0-1} = 0.36$ eV), whereas the nonadiabatic contribution exhibits no translational incidence energy threshold.

DISCUSSION

It is now possible to discern trends in the propensity for vibrational inelasticity for seven molecule–surface scattering systems. Figure 4 shows one means of comparison, where only the electronically nonadiabatic nature of the vibrationally inelastic scattering is represented. In all cases, the electronically adiabatic contribution to vibrational inelasticity is either negligible, or it has been accounted for and removed. Referring to Eq. (2), this means that either $A_{0,1}^{ad.}(E_i) \ll A_{0,1}^{nonad.}(E_i)$ or that both of these coefficients have been experimentally determined. In Fig. 4, $A_{0,1}^{nonad.}(E_i)$ is plotted logarithmically vs $\langle E_i \rangle$. The purpose of the right panel in Fig. 4 is to remind the reader of the energetics for electron transfer in each system, which are closely related to the difference of the molecule's electron affinity (EA) and the solid's work function.

The first thing we notice about Fig. 4 is that in all cases, increasing E_i leads to larger values of $A_{0,1}^{nonad.}(E_i)$. This can be qualitatively understood as an incidence energy dependent variation of the distance of closest approach of the molecule to the surface, resulting in increased image charge stabilization of the charge transferred state at closer distance to the surface and stronger coupling of the neutral and anion states.

We also notice that the various scattering systems order themselves roughly on this plot according to the energetics of electron transfer. Those systems where EA $\ll \Phi$ exhibit small values of $A_{0,1}^{nonad.}(E_i)$, whereas those where the difference is smaller exhibit substantially larger values of $A_{0,1}^{nonad.}(E_i)$. However, this correlation is not perfect. Note, for example, that while EA–Φ for HCl/Au lies midway on the scale, its $A_{0,1}^{nonad.}(E_i)$ values are some of the smallest seen in any system. Specifically, EA–Φ for HCl/Ag is actually larger than that of NO/Au, yet the former exhibits electronically nonadiabatic vibrational inelasticity less than the latter.

This is probably due to the differences in the interaction potentials of the two systems that control the distance of closest approach. The van der Waals radii of N (1.66 Å), O (1.50 Å), and Cl (1.82 Å)[26] suggest that the distance of closest approach for HCl could be larger than that of NO. DFT calculations predict the distance of closest approach is systematically larger for HCl than for NO scattering from noble metals as long as HCl is not oriented properly or strikes far from the reactive site for dissociation. See potential energy surfaces reported for NO/Au(111),[35,36] HCl/Au(111),[37–40] and HCl/Ag(111).[41] A change in the distance of closest approach of ~0.2 Å can alter the image charge stabilization by several hundred meV.[23] While this influence produces a shift of $A_{0,1}^{nonad.}(E_i)$ that has the right sign, it may not be enough to explain the magnitude of the differences seen in Fig. 4. Of course, the HCl molecule also has about 20% more mass than NO and thus at the same incidence energy, represents accordingly reduced speed. The degree to which the BOA fails is obviously a question of time scales: hence, this also is an important factor.

Both HCl/Au and HCl/Ag are different from the other systems represented in Fig. 4 in that they exhibit substantial adiabatic contributions to the vibrational inelasticity; in both cases, $A_{0,1}^{ad.}(E_i) \sim 0.01 \times A_{0,1}^{nonad.}(E_i)$. This is in all likelihood due to the low energy barrier to dissociation present in both of these systems.[37–47] Electronically adiabatic vibrational excitation has been studied for H_2 on Cu[48–50] and N_2 on Ru(0001)[51]—in both cases, the "elbow" potential associated with dissociative adsorption is seen to promote translational to vibrational energy transfer. We expect similar dynamics are present for HCl on Ag and Au, if HCl is oriented correctly and attacks at the proper surface site to allow approach to the transition state. In fact, first principles calculations of vibrational excitation of HCl on Au show trajectories that approach the transition state for dissociative adsorption but fail to react, often resulting in T–V energy transfer.[46]

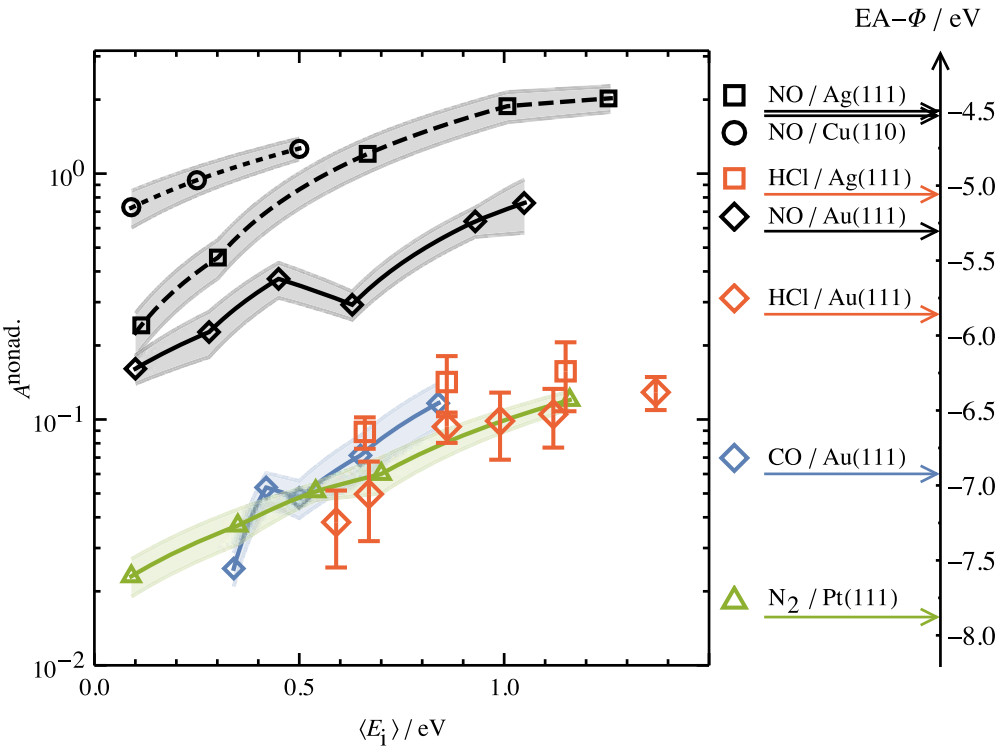

FIG. 4. Nonadiabatic interaction strengths for vibrational excitation in several molecule/surface systems. On the left-hand side, the nonadiabatic interaction strength $A^{\text{nonad.}}$ is shown depending on the mean incidence translational energy $\langle E_i \rangle$. Open symbols depict excitations from the ground vibrational state to the first excited state. Interpolating lines in the same color act as a guide to the eye, and correspondingly shaded areas depict associated uncertainties. On the right-hand side, molecule/surface-systems are ranked according to the difference of the metal's work function Φ and the molecule's electron affinity (EA). Based on its position on this scale, the $v = 0 \rightarrow 1$ interaction strength of HCl on Au(111) and Ag(111) is relatively low. On the other hand, the nonadiabatic interaction for the hot band excitation $v = 1 \rightarrow 2$ on Au(111) is strong compared to the ground state excitation on Au(111) as well as NO ($v = 2 \rightarrow 3$)/Au(111). While $A^{\text{nonad.}}$ was calculated from data in Refs. 12, 15, 17, 20, and 22, values for work functions were taken from Ref. 28 and electron affinities were taken from Ref. 55.

It is also interesting to consider electronically nonadiabatic vibrationally inelastic scattering of vibrationally pre-excited molecules. For example, for HCl ($v = 1 \rightarrow 2$) in scattering from Au(111), $A^{\text{nonad.}}$ is 8× larger than that for HCl ($v = 0 \rightarrow 1$). By comparison, NO ($v = 2 \rightarrow 3$) transitions seen in NO scattering from Au(111)[16,27,52] exhibit an $A^{\text{nonad.}}$ that is only 2× larger than that of NO ($v = 0 \rightarrow 1$). If we consider the behavior of a simple harmonic oscillator within the framework of Landau and Teller,[53,54] we would expect $P_{v_{\text{final}},v_{\text{initial}}}$ to scale with $(v_{\text{initial}} + 1)$: a 2-fold enhancement for HCl ($v = 1 \rightarrow 2$) vs HCl ($v = 0 \rightarrow 1$) and a 3-fold enhancement for NO ($v = 2 \rightarrow 3$) vs NO ($v = 0 \rightarrow 1$). The fact that HCl exhibits an 8-fold enhancement for HCl ($v = 1 \rightarrow 2$) vs HCl ($v = 0 \rightarrow 1$) is likely due to the more anharmonic HCl/Au PES in comparison to NO/Au resulting from a low energy barrier to H–Cl dissociation. The existence of a low dissociation barrier may also allow the HCl molecule to approach more closely to the surface affecting image charge stabilization and enhancing electron transfer related nonadiabatic coupling.

These effects discussed for HCl/Au appear also to be present for HCl/Ag. The important role of electronically adiabatic vibrational inelasticity, for example, suggests the influence of the dissociative adsorption transition state. It is also interesting that HCl ($v = 1 \rightarrow 2$) scattering from Ag(111) could not be observed. Apparently, the dissociative adsorption probability for HCl ($v = 2$) is large, as suggested by recent DFT calculations.[44] We postulate that scattering events where HCl ($v = 1$) is subject to dynamical influences that increase its vibrational energy lead efficiently to dissociation before the HCl ($v = 2$) molecule can escape the surface. We emphasize that, while this hypothesis is reasonable and the observations are unambiguous, further work is needed to confirm this line of thinking.

SUMMARY AND CONCLUSIONS

We have shown that the $v = 0 \rightarrow 1$ excitation of HCl molecules scattered from Ag(111) results from interactions that are both electronically adiabatic—T–V energy transfer—as well as electronically nonadiabatic—Born–Oppenheimer failure where vibration couples to metal electrons. We observe a larger influence of electronic nonadiabaticity compared to the previously reported HCl/Au(111) system—this results from the lower work function of Ag compared to Au, which leads to more efficient production

of a transient HCl^-. Unlike the HCl/Au(111) system, vibrationally inelastic $v = 1 \rightarrow 2$ transitions could not be seen when HCl ($v = 1$) collides with an Ag(111) surface. We suggest that scattering events, where HCl ($v = 1$) is subject to dynamical influences that increase its vibrational energy, lead efficiently to dissociation before the HCl ($v = 2$) molecule can escape the surface, making it an excellent candidate to study electronically nonadiabatic effects in dissociative adsorption.

ACKNOWLEDGMENTS

We acknowledge support from the Deutsche Forschungsgemeinschaft under Project No. WO 1541/9-1. J.G. acknowledges support from the Max-Planck–EPFL Center for Molecular Nanoscience and Technology. The authors would also like to thank Dr. Geert-Jan Kroes for stimulating discussions and Dr. Alexander Kandratsenka for his insights into computational chemistry.

DATA AVAILABILITY

The data that support the findings of this study are available from the corresponding author upon reasonable request.

REFERENCES

[1] M. Born and R. Oppenheimer, Ann. Phys. **389**, 457 (1927).
[2] J. D. White *et al.*, Nature **433**, 503 (2005).
[3] H. Nienhaus *et al.*, Phys. Rev. Lett. **82**, 446 (1999).
[4] B. Gergen *et al.*, Science **294**, 2521 (2001).
[5] B. Mildner, E. Hasselbrink, and D. Diesing, Chem. Phys. Lett. **432**, 133 (2006).
[6] B. Schindler, D. Diesing, and E. Hasselbrink, J. Phys. Chem. C **117**, 6337 (2013).
[7] O. Bünermann *et al.*, Science **350**, 1346 (2015).
[8] Y. Dorenkamp *et al.*, J. Chem. Phys. **148**, 034706 (2018).
[9] H. Jiang *et al.*, J. Chem. Phys. **150**, 184704 (2019).
[10] A. Kandratsenka *et al.*, Proc. Natl. Acad. Sci. U. S. A. **115**, 680 (2018).
[11] C. T. Rettner *et al.*, Phys. Rev. Lett. **55**, 1904 (1985).
[12] C. T. Rettner *et al.*, Surf. Sci. **192**, 107 (1987).
[13] B. C. Krüger *et al.*, J. Phys. Chem. Lett. **7**, 441 (2016).
[14] C. Steinsiek *et al.*, J. Phys. Chem. C **122**, 10027 (2018).
[15] E. K. Watts, J. L. W. Siders, and G. O. Sitz, Surf. Sci. **374**, 191 (1997).
[16] Y. Huang *et al.*, Phys. Rev. Lett. **84**, 2985 (2000).
[17] R. Cooper *et al.*, J. Chem. Phys. **137**, 064705 (2012).
[18] C. T. Rettner, J. Chem. Phys. **99**, 5481 (1993).
[19] T. Schäfer *et al.*, Phys. Chem. Chem. Phys. **15**, 1863 (2013).
[20] P. R. Shirhatti *et al.*, J. Chem. Phys. **141**, 124704 (2014).
[21] R. J. V. Wagner *et al.*, J. Phys. Chem. Lett. **8**, 4887 (2017).
[22] J. Werdecker *et al.*, J. Phys. Chem. C **119**, 14722 (2015).
[23] R. J. V. Wagner *et al.*, Phys. Chem. Chem. Phys. **21**, 1650 (2019).
[24] Y. Huang *et al.*, Science **290**, 111 (2000).
[25] J. D. D. Martin and J. W. Hepburn, J. Chem. Phys. **109**, 8139 (1998).
[26] S. Alvarez, Dalton Trans. **42**, 8617 (2013).
[27] J. Geweke *et al.*, J. Chem. Phys. **145**, 054709 (2016).
[28] G. N. Derry, M. E. Kern, and E. H. Worth, J. Vac. Sci. Technol., A **33**, 060801 (2015).
[29] Q. Ran *et al.*, Rev. Sci. Instrum. **78**, 104104 (2007).
[30] I. Rahinov *et al.*, J. Chem. Phys. **129**, 214708 (2008).
[31] K. Golibrzuch *et al.*, J. Chem. Phys. A **117**, 8750 (2013).
[32] P. R. Shirhatti *et al.*, J. Phys. Chem. Lett. **7**, 1346 (2016).
[33] Q. Ran *et al.*, Phys. Rev. Lett. **98**, 237601 (2007).
[34] B. D. Kay, T. D. Raymond, and M. E. Coltrin, Phys. Rev. Lett. **59**, 2792 (1987).
[35] S. Roy, N. A. Shenvi, and J. C. Tully, J. Chem. Phys. **130**, 174716 (2009).
[36] R. Yin, Y. Zhang, and B. Jiang, J. Phys. Chem. Lett. **10**, 5969 (2019).
[37] T. Liu, B. Fu, and D. H. Zhang, Sci. China Chem. **57**, 147 (2013).
[38] G. Füchsel *et al.*, J. Phys. Chem. C **120**, 25760 (2016).
[39] B. Kolb *et al.*, J. Phys. Chem. Lett. **8**, 666 (2017).
[40] Q. Liu *et al.*, J. Phys. Chem. C **122**, 1761 (2018).
[41] T. Liu, B. Fu, and D. H. Zhang, J. Chem. Phys. **149**, 054702 (2018).
[42] T. Liu, B. Fu, and D. H. Zhang, J. Chem. Phys. **139**, 184705 (2013).
[43] T. Liu, B. Fu, and D. H. Zhang, J. Chem. Phys. **146**, 164706 (2017).
[44] T. Liu, B. Fu, and D. H. Zhang, J. Chem. Phys. **149**, 174702 (2018).
[45] T. Liu, B. Fu, and D. H. Zhang, J. Chem. Phys. **151**, 144707 (2019).
[46] N. Gerrits *et al.*, J. Phys. Chem. C **124**, 15944 (2020).
[47] G. Füchsel *et al.*, J. Phys. Chem. C **123**, 2287 (2019).
[48] D. Halstead and S. Holloway, J. Chem. Phys. **93**, 2859 (1990).
[49] C. T. Rettner, D. J. Auerbach, and H. A. Michelsen, Phys. Rev. Lett. **68**, 2547 (1992).
[50] C. T. Rettner, H. A. Michelsen, and D. J. Auerbach, J. Chem. Phys. **102**, 4625 (1995).
[51] C. Diaz and R. A. Olsen, J. Chem. Phys. **130**, 094706 (2009).
[52] A. M. Wodtke, Y. Huang, and D. J. Auerbach, Chem. Phys. Lett. **364**, 231 (2002).
[53] L. Landau and E. Teller, Phys. Z. Sow. **10**, 34 (1936).
[54] E. E. Nikitin and J. Troe, Phys. Chem. Chem. Phys. **10**, 1483 (2008).
[55] R. D. Johnson III, NIST Standard Reference Database Number 101, Release 18, 2016.